Indian J Phys (October 2016) 90(10):1127–1132
DOI 10.1007/s12648-016-0856-3

ORIGINAL PAPER

A new approach to study the effect of generation rate on drain-source current of bilayer graphene transistors

H Ahmad[1], M Ghadiry[1]* and A AbdManaf[2]

[1]Photonics Research Centre, University of Malaya, 50603 Kuala Lumpur, Malaysia

[2]Collaborative Microelectronic Design Excellence Center (CEDEC), School of Electrical and Electronic Engineering, Universiti Sains Malaysia, 11900 Bayang Lepas, Pulau Pinang, Malaysia

Received: 23 September 2015 / Accepted: 27 January 2016 / Published online: 28 April 2016

Abstract: This paper presents a new approach to study the effect of impact ionization on the current of bilayer graphene field effect transistors. Analytical models for surface potential and current together with a Monte Carlo approach which include the edge effect scattering are used to calculate the current and generation rate in bilayer graphene transistors due to ionization. FlexPDE simulation is also employed for verification of surface potential modeling. Using the approach, the profile of generation rate, surface potential and current are plotted with respect to several structural parameters. We have shown that ignoring this effect in the modeling will result in an error of up to 10 % for a typical 30 nm bilayer graphene field effect transistor. As a result, we conclude that any analytical study ignoring the ionization is incomplete for bilayer graphene field effect transistors. The model presented here can be applied in optimization of photo detectors based on graphene.

Keywords: Graphene; Field effect transistor; Carrier generation; Modelling; Monte Carlo; Graphene photo detector

PACS Nos.: 81.05.ue; 72.20.-I; 85.30.Tv; 34.80.Dp

1. Introduction

In the last few years, graphene with extraordinary physical properties such as its two dimensional (2D) nature, semi-linear band structure, tunable bandgap and low effective mass (therefore, high velocity of carriers) has found its use in many electronic applications [1–4]. As a result, a great amount of research has been conducted to explore new insights into the electrical and physical properties of this new material and to find out its potential applications [5–8]. In this context, graphene's 2D nature and high carrier velocity are well studied for high speed and high performance electronics. In addition, the interaction between charge carriers and static and dynamic lattice defects has been taken into account in calculations [9, 10]. However, in depth study on the interband interaction between carriers has not been carried out. One of the most important contributors in carrier generation is ionization [11–14]. In conventional semiconductors, ionization threshold energy, which is the energy a carrier needs to travel from the valence band to the conduction band, dictates the ionization probability. Only carriers gaining enough energy (more than the ionization threshold energy) from external electric field could pass the barrier and be ionized. This energy is of the order of the bandgap. Therefore, for gapless graphene, this energy is not defined, whereas for bilayer graphene, (BLG), it could be calculated [15, 16]. Recently, it is shown that at constant carrier temperature strongly decreases with the carrier concentration as it reduces the density of final scattering states for both carriers [17]. Due to the small bandgap of BLG, it seems that the ionization rate is high and its effect on current is significant. Therefore, we believe that any study of the transport characteristics and current–voltage (I–V) characteristics of BLG without the consideration of impact ionization is incomplete. As a result, in this paper, we calculate the ionization rate as a major contributor in carrier generation rate in BLG and include its effect in the modelling of drain current to explore its importance in the I–V characteristics of BLG field effect transistors (BLGFET).

*Corresponding author, E-mail: mahdiar@um.edu.my

2. The proposed approach

A cross sectional view of a double gate BLGFET and the definition of the geometrical characteristics are depicted in Fig. 1. In the device structure, t_{ox} is the oxide thickness of the top and back gates, t_{ch} is the BLG channel thickness, t_g is the thickness of a single graphene layer, t_d is the distance between the two graphene layers, V_{tg} and V_{bg} are respectively the front and back gate biases, and V_{ds} is the drain-source voltage.

Consider a BLG in a lateral electric field F (toward the y direction in Fig. 1), the current densities of holes and electrons in steady state have the following relation with the impact ionization generation rate

$$\frac{d(J_p - J_n)}{dy} = 2Gq \tag{1}$$

where J_p and J_n are the current densities of holes and electrons respectively, q is the electron charge, and G is the electron generation rate due to impact ionization. According to the definition of the ionization coefficient and considering only electrons generated by electrons, the generation rate is given by [12]

$$G = v_d n_i \alpha \tag{2}$$

where v_d is drift velocity, n_i is intrinsic carrier concentration of BLG and α is the ionization rate. Integration of Eq. (1) results in

$$I_p - I_n - 2qW \int_y^L G dy = I \tag{3}$$

where I is the total channel current, and I_n and I_p are the electron and hole currents respectively. Considering the positive gate-source voltage and negative channel, the electron charge is given by $Q = C_G(V_{gt} - V_{bg} - \varphi(y))$ where $\varphi(y)$ is the surface potential and the electron current is defined as $I = QWv_d(F)$ where W is the BLG channel width, F is the lateral electric field, and

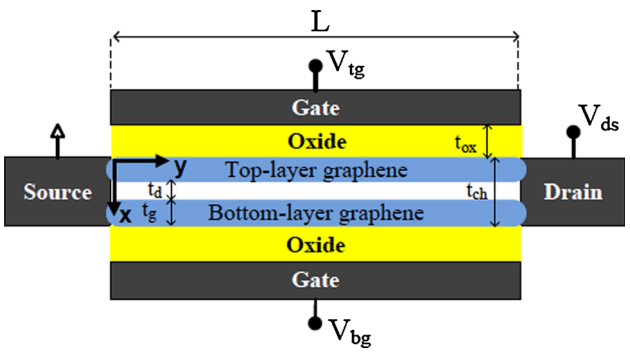

Fig. 1 Cross sectional view of bilayer graphene double gate transistor

$$v_d = \frac{\mu F(y)}{1 + F(y)/F_C} \tag{4}$$

is the carrier velocity [13], where μ is mobility and F_C is the critical electric field (the drain current saturates when electric field exceeds this value). Using charge equation, one can write

$$C_G W(V_{gt} - V_{bg} - \varphi(y))v_d + 2qW \int_0^y G dy = I \tag{5}$$

where the gate capacitance is calculated from $C_G = C_q C_{ox}/C_q + C_{ox}$ [18], C_{ox} and C_q are classic and quantum capacitances of the gate given by $C_{ox} = \varepsilon_{ox}/t_{ox}$ and $C_q = 2$ μF/cm^2, respectively with ε_{ox} being oxide dielectric constant. Therefore, the drain current equation could be written by integrating from source ($y = 0$) to position y along the channel over Eq. (5). As a result, we have

$$I = \frac{C_g W \mu}{1 + \left(\frac{\varphi(y)}{F_C}\right)}\left(\left(V_{tg} - V_{bg} - \frac{V_{DS}}{2}\right)V_{DS}\right) + \frac{2qWG}{1 + \left(\frac{\varphi(y)}{F_C}\right)}\left(L\left(L + \frac{V_{DS}}{F_C}\right) - \int_0^L \left(y + \frac{\varphi(y)}{F_c}\right)dy\right) \tag{6}$$

which is calculated numerically. To find out how important the generation rate is in the current of BLGFETs at different situations, we ignore the effect of carrier generation in the model. We start the modeling by $I_p - I_n = I$. Then, we have

$$C_g W(V_{tg} - V_{bg} - \varphi(y))v_d = I \tag{7}$$

As a result, the current is written as

$$I = \frac{F_c \cdot W}{F_c + \varphi(y)}\left(C_g \mu\left(V_{tg} - V_{bg} - \frac{V_{DS}}{2}\right)\varphi(y)\right) \tag{8}$$

According to [19], the surface potential in BLG could be given as

$$\varphi(x, y) = D_{21}\exp(\sqrt{\alpha_2}y) + D_{22}\exp(-\sqrt{\alpha_2}y) - \frac{\beta_2}{\alpha_2} \tag{9}$$

where

$$D_{21} = \upsilon_{S2} + \frac{\upsilon_{D2} - \upsilon_{S2}\exp(\sqrt{\alpha_2}L)}{exp(\sqrt{\alpha_2}L) - \exp(-\sqrt{\alpha_2}L)} \tag{10}$$

$$D_{22} = \frac{\upsilon_{S2}\exp(\sqrt{\alpha_2}L) - \upsilon_{D2}}{exp(\sqrt{\alpha_2}L) - \exp(-\sqrt{\alpha_2}L)} \tag{11}$$

$$\upsilon_{S2} = V_{bi} + \frac{\beta_2}{\alpha_2} \tag{12}$$

$$\upsilon_{D2} = V_{bi} + V_{ds} + \frac{\beta_2}{\alpha_2} \tag{13}$$

where V_{bi} is the built in voltage of BLG calculated according to [19] and α_2 and β_2 are defined as

$$\alpha_2 = \frac{C_g\left(2 + t_{ch} + \frac{C_0 t_{ch}}{\varepsilon_g}\right)}{A\left(1 + \frac{C_g}{\varepsilon_g}x' - \frac{C_g(1+D)}{A}x'^2\right)} \tag{14}$$

$$\begin{aligned}\beta_2 = {} & \frac{q(N_D + n_i)}{\varepsilon_g} - C_g\left(DV'_{tg} - V'_{bg}\right) + C_0 K \\ & + \left(\frac{C_g V'_{tg} - C_0 K}{\varepsilon_g}\right)\alpha^2 x' \\ & - \left(\frac{C_g\left(DV'_{tg} + V'_{bg}\right) - C_0 KD}{A}\right)\alpha_2 x'^2\end{aligned} \tag{15}$$

For calculation of k, D, C_0, V'_{tg} and V'_{bg} please refer to ref [19].

3. Monte Carlo simulation for calculation of generation rate

Among several scattering mechanisms influencing the carriers in graphene, three dominant mechanisms, which are the acoustic phonons, optical phonons and edge effect, are considered in this simulation [12]. Inelastic scattering (energy relaxing collisions) results in the release of energy $\hbar\omega_{op}$. The respective scattering rates are calculated based on the associated mean free paths $\lambda_m = \upsilon_F \tau_m$ and λ_E and λ_{edge} being the momentum, energy and edge scattering mean free paths respectively. The energy mean free path is written as [12]

$$\lambda_E = \frac{E\tau_m \upsilon_g}{\hbar\omega_{op}\upsilon_F} \tag{16}$$

with E being the carrier energy, w_{op} the optical phonon frequency and V_g the group velocity of carriers. It is assumed that the impact ionization happens immediately after the carriers gain enough kinetic energy, which is greater than the ionization threshold energy E_t [20]. We use a self-scattering approach, which introduces a fictitious forward scattering in order to eliminate solving integral equations in every Monte Carlo step. The R_{ss}, which is the self-scattering rate, is calculated from $R_{ss} = \upsilon_g/\lambda$, where $\lambda = \frac{1}{m} + \frac{1}{\lambda_E} + \frac{1}{\lambda_{edge}}$. The group velocity is calculated from [21]

$$\upsilon_g = \frac{2}{\pi\hbar DoS} \tag{17}$$

where $\hbar$ is the reduced Plank's constant and DOS is the density of the states. The edge scattering mean free path according to [22] is given as

$$\lambda_{edge} = \frac{w}{p_{back}}\sqrt{\left(1 + \frac{2E}{E_g}\right)^2 - 1} \tag{18}$$

where E is calculated from $E_k = \hbar^2\boldsymbol{k}^2/m^*$, E_g bandgap energy and P_{back} is the probability of back-scattering which depends on edge quality of samples [23]. From [24], a backscattering probability of $P_{back} < 20\ \%$ is suggested. Ballistic flight time (dt) is obtained from $dt = -1/R_{ss}\ln(r)$ where r is a number between 0 and 1 chosen randomly. The position vector $\boldsymbol{X}$ and wavevector $d\boldsymbol{k}$ are written as

$$d\boldsymbol{X} = \boldsymbol{k}\frac{\hbar dt}{m} + \frac{q\boldsymbol{F}dt^2}{2m} \tag{19}$$

and

$$d\boldsymbol{k} = q\boldsymbol{F}dt/\hbar \tag{20}$$

respectively. For elastic or inelastic scatterings, the orientation of $\boldsymbol{k}$ is changed, whereas for self-scatterings, $\boldsymbol{k}$ remains unchanged. The ionization rate is given as $\alpha = 1/Z$ [24], where Z is the average distance the carriers travel before reaching ionization energy.

4. Typical values for simulation

Now the model is complete and ready for calculation. Device parameters are given in Table 1.

Using Eqs. (6) and (8), the device current can be calculated with and without considering the effect of ionization with the help of Monte Carlo simulation.

Table 1 Device parameters used in simulation and modelling

Symbol	Description	Value
υ_g	Group velocity	$\sim 3.4 \times 10^6$ m/s
λ_m	Average momentum mean free path	35 nm
n_i	Intrinsic carrier concentration	5×10^{13} 1/cm^2
$\hbar$	Reduced Planck's constant	$6.6 \times 10^{-34}/2\pi$ J s
$\hbar\omega_{op}$	Phonon energy	0.2 eV
q	Charge magnitude	1.6×10^{-19} C
w	Channel width	20 and 30 nm
L	Channel length	20 nm
m	Free electron effective mass	9.11×10^{-31} kg
V_{gt}	Top gate voltage	0.4–0.8 V
V_{bg}	Back gate voltage	0.4–0.8 V
t_{si}	Si substrate thickness	200 nm
t_{CH}	GNR (channel) thickness	1.3 nm
t_{OX}	Oxide thickness	1 nm
T	Temperature	300–500 K
N_D	Doping concentration	1×10^{12} 1/cm^2

5. Results and discussion

The ionization coefficient values for BLG with respect to low electric field for three different values of interlayer potential energies, $U = qV$, where V is the interlayer voltage induced by gate voltage, is depicted in Fig. 2. The simulation results of the proposed model for BLG are compared with the simulation data of silicon extracted from [25]. Although the values for BLG are higher than those of silicon over the range of electric field used in the simulation, it can be seen that the profile is the same for both.

Using Gaussian software, the threshold energy of ionization can be calculated [11]. From Fig. 3, it can be seen that for conventional semiconductors, the threshold energy of ionization is a function of the potential difference of the layers in BLG, and for higher interlayer potentials the threshold energy increases. Moreover, the larger threshold energy means electrons need more energy to achieve impact ionization, resulting in smaller ionization coefficient.

Thus, the interlayer potential of BLG can be considered as a tuning parameter for its ionization coefficient, which is shown in Fig. 4. The ionization coefficient of BLG is illustrated at high electric fields with temperature and

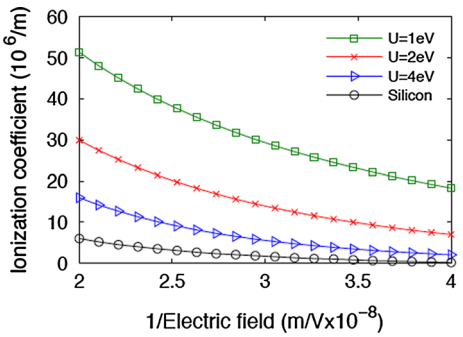

Fig. 2 Ionization coefficient of BLG versus low range electric field for three different interlayer potential energies. The simulation results of silicon are extracted from Fig. 5 of [25]

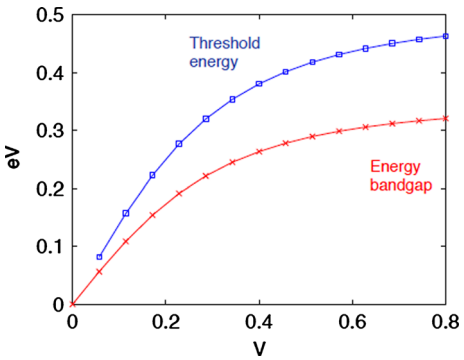

Fig. 3 Threshold energy and energy bandgap of BLG versus interlayer potential

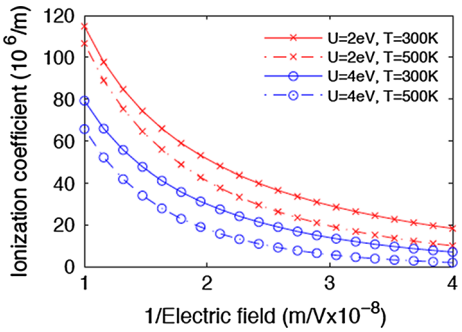

Fig. 4 Ionization coefficient of BLG versus electric field (including high ranges) for two values of interlayer potential energies and temperatures

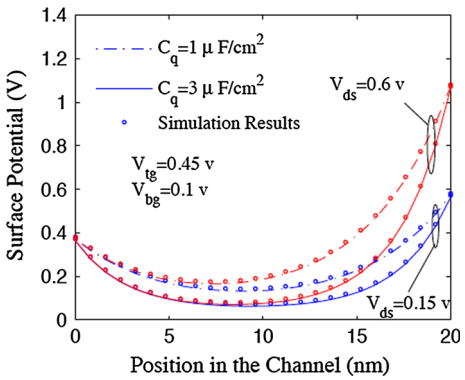

Fig. 5 Analytical and simulation results of the front side (x = 0) potential distribution along the channel with $t_{ox} = 1$ nm, $L = 20$ nm, $N_D = 1\ e^{12}$ cm^{-2}, $n_i = 1\ e^{13}$ cm^{-2}. The obtained results of the analytical model are represented by lines and the FlexPDE simulation results are represented by symbols

interlayer potential as variables. Increasing the temperature results in more collisions, and that in turn reduces the velocity of carriers. Therefore, the carriers can only reach the threshold energy at stronger electric fields.

Using FlexPDE, the surface potential can be simulated. However, we have preferred to use the surface potential model presented in [26], which is simpler and quicker for our calculations. We first verify the surface potential model, after which we use it in our model. 2-D Poisson's equation of the front side potential (x = 0) along the channel is numerically solved using the FlexPDE 5.0. In Fig. 5, the calculated results of the analytical model (represented by lines) and the simulation results of the FlexPDE (represented by symbols) at the top gate interface are illustrated versus the position in the channel for two values of the drain-source voltage ($V_{ds} = 0.15$ and 0.6 V), and two values of the quantum capacitance ($C_q = 1$ and 3 μF/cm^2). Evidently, a good agreement is obtained between the analytical and numerical results, which represents the validity of the model within the simulation parameters used. Since the quantum capacitance in bilayer

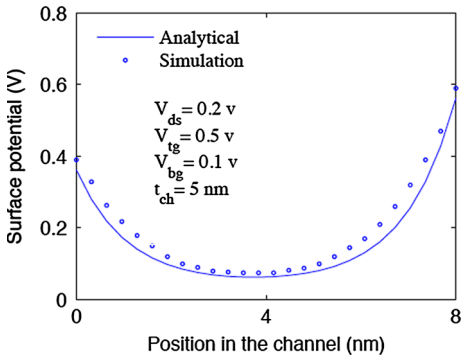

Fig. 6 The front side ($x = 0$) potential distribution along the channel for channel width comparable with channel length, with $t_{ox} = 1$ nm, $L = 8$ nm, $N_D = 1$ e^{12} cm^{-2}, $n_i = 1$ e^{13} cm^{-2}

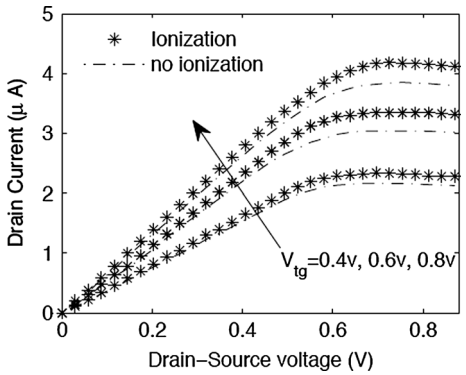

Fig. 7 Drain current with and without considering the generation rate as a function of drain-source voltage for different values of back gate voltages

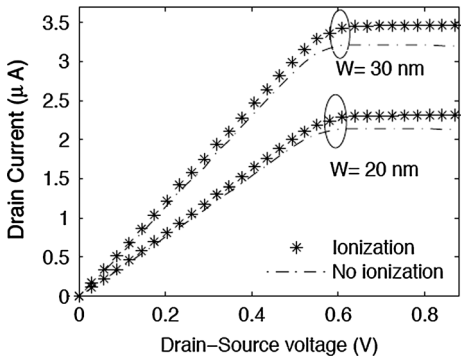

Fig. 8 Drain current with and without considering the generation rate as a function of drain-source voltage for different channel width

graphene is directly proportional to the carrier concentration and is inversely proportional to the energy band gap [27], the potential along the channel can be controlled through the carrier density and applied voltage to the gates. We can see that the surface potential values are considerably changed for two values of the quantum capacitance. The reason is that the gate oxide capacitance is much larger than the quantum capacitance for BLG due to its low density of state. Therefore the value of C_G is limited by C_q.

It is worth mentioning that Fig. 5 shows the results for $L \gg t_{ch}$. As the electric field near to the drain and source contacts is more intense, the scenario is different when the channel length is reduced and it is comparable to the oxide thickness. In this case, the electric field distribution is not uniform along the front and back gate interfaces, and the non-vertical electric field is developed near the middle of the channel. Hence, the boundary conditions of solving surface potential are not accurate any more, which disrupt the agreement between the simulation and analytical results. The analytical and simulation results are illustrated in Fig. 6 for $L = 8$ nm and $t_{ch} = 5$ nm.

Using the proposed current model, the effect of ionization on drain-source current can now be studied. Fig. 7 shows the results. The dashed-lines show the result of modeling when the effect of carrier generation is ignored, while the points are the results from the model with the effect of carrier generation included. To examine the effect of the carrier generation, the width of the BLG channel is changed and the results are shown in Fig. 8. The difference of drain currents with and without consideration of generation rate increases when the channel width increases. As the width increases, the bandgap decreases and the carrier generation increases. From both figures, it is seen that by ignoring the effect of ionization, calculation of drain source current in BLG- FETs could lead to an error of up to 10 %, which is significant in modelling. Therefore, it is suggested that in any analytical study of nanoscale BLGFET, the effect of ionization should be included.

6. Conclusion

In this paper, we have proposed two models to study the effect of the carrier generation in the current-voltage characteristic of bilayer graphene (BLG) field effect transistors. The models are based on surface potential and generation rate. The surface potential is calculated analytically and the generation rate is obtained by Monte Carlo simulation. Surface potential model is verified using FlexPDE simulation. The effect of generation rate on drain-source current are studied. We show that generation rate in BLG is strong and it is almost five times greater than that of silicon. In addition, it is shown that for BLG ignoring ionization results in an error rate of up to 10 %, which is significant in modelling. In addition, we show that the generation rate and ionization threshold voltage are functions of layer voltage and tunable. The presented model in this paper is based on a general method and can be used in other applications such as design and optimization of avalanche photo diodes, which relies on the effect of impact ionization.

Acknowledgments We would like to acknowledge the full support from University of Malaya through their Funding LRGS(2015) NGOD/um/KPT, RP029A-15AFR, RU007/2015 and GA010-2014(ulung).

References

[1] M N Senejani, M Ghadiry, C Y Ooi and M N Marsono, *Circuits Syst. Signal Process.* **34** 4 (2015)
[2] M Khaledian, R Ismail, M Saeidmanesh, M Ghadiry and E Akbari, *Plasmonics* **10** 1133 (2015)
[3] M Rahmani, M Ahmadi, R Ismail and M Ghadiry, *J. Comput. Theor. Nanosci.* **10** 2 (2013)
[4] K Novoselov, A K Geim, S Morozov, D Jiang, M Katsnelson, I Grigorieva, S Dubonos and A Firsov, *Nature* **438** 7065 (2005)
[5] A K Geim and K S Novoselov, *Nat. Mater.* **6** 3 (2007)
[6] M Rahmani, M Ahmadi, M Ghadiry, J Samadi, S Anwar and R Ismail, *J. Comput. Theor. Nanosci.* **9** 10 (2012)
[7] H K F Abadi, M Ahmadi, R Yusof, M Saeidmanesh, M Rahmani, M J Kiani and M Ghadiry, *Sci. Adv. Mater.* **6** 3 (2014)
[8] M Ghadiry, A A Manaf, M T Ahmadi, H Sadeghi and M N Senejani, *J. Nanomater.* **2011** (2011)
[9] P Khomyakov, G Giovannetti, P Rusu, G Brocks, J Van den Brink and P Kelly, *Phys. Rev. B* **79** 19 (2009)
[10] J Yan, Y Zhang, P Kim and A Pinczuk, *Phys. Rev. Lett.* **98** 16 (2007)
[11] M Ghadiry, A B A Manaf, M Nadi, M Rahmani and M Ahmadi, *Microelectron. Reliab.* **52** 7 (2012)
[12] M Ghadiry, A B A Manaf, M Nadi, M Rahmani and M T Ahmadi, *Microelectron. Reliab.* **52** 7 (2012)
[13] M Saeidmanesh, M Ghadiry, M Khaledian, M Kiani and R Ismail, *J. Comput. Electron.* **13** 1 (2014)
[14] F Rana, *Phys. Rev. B* **76** 15 (2007)
[15] F Xia, D B Farmer, Y-m Lin and P Avouris, *Nano Lett.* **10** 2 (2010)
[16] M Saeidmanesh, M Ahmadi, M Ghadiry, E Akbari, M Kiani and R Ismail, *J. Comput. Theor. Nanosci.* **10** 9 (2013)
[17] L Pirro, A Girdhar, Y Leblebici and J-P Leburton, *J. Appl. Phys.* **112** 9 (2012)
[18] I Meric, M Y Han, A F Young, B Ozyilmaz, P Kim and K L Shepard, *Nat. Nanotechnol.* **3** 11 (2008)
[19] M Saeidmanesh, M Rahmani, H Karimi, M Khaledian and R Ismail, *Microelectron. Reliab.* **54** 1 (2014)
[20] W-D Park and K Tanioka, *Jpn. J. Appl. Phys.* **53** 3 (2014)
[21] M Bresciani, A Paussa, P Palestri, D Esseni and L Selmi, Low-field mobility and high-field drift velocity in graphene nanoribbons and graphene bilayers, in *Electron Devices Meeting (IEDM), 2010 IEEE International*, 2010, pp. 32.1.1–32.1.4.
[22] X Wang, Y Ouyang, X Li, H Wang, J Guo and H Dai, *Phys. Rev. Lett.* **100** 20 (2008)
[23] V Ryzhii, A Satou, M Ryzhii, T Otsuji and M Shur, *J. Phys. Condens. Matter* **20** 38 (2008)
[24] O Rubel, A Potvin and D Laughton, *J. Phys. Condens. Matter* **23** 5 (2011)
[25] K Yeom, J Hinckley and J Singh, *J. Appl. Phys.* **80** 12 (1996)
[26] M Saeidmanesh, M Kiani, K E Siew, E Akbari, H Karimi and R Ismail, *J. Nanomater.* **2013** (2013)
[27] J Xia, F Chen, J Li and N Tao, *Nat. Nanotechnol.* **4** 8 (2009)